Early Focal Expression of the Chemokine Ccl2 by Müller Cells during Exposure to Damage-Inducing Bright Continuous Light

Matt Rutar,[1,2] *Riccardo Natoli,*[1,3] *Krisztina Valter,*[1,2] *and Jan M. Provis*[1,2,3]

Purpose. To investigate the time course and localization of Ccl2 expression and recruitment of inflammatory cells associated with light-induced photoreceptor degeneration.

Methods. Sprague-Dawley (SD) rats were exposed to 1000 lux light for up to 24 hours, after which some animals were allowed to recover in dim light (5 lux) for 3 or 7 days. During and after exposure to light, the animals were euthanized and the retinas processed. Ccl2 expression was assessed by qPCR, immunohistochemistry, and in situ hybridization at each time point. Counts were made of perivascular monocytes/microglia immunolabeled with ED1, and photoreceptor apoptosis was assessed with TUNEL.

Results. Upregulation of Ccl2 expression was evident in the retina by 12 hours of exposure and correlated with increased photoreceptor death. Ccl2 expression reached its maximum at 24 hours, coinciding with peak cell death. Immunohistochemistry and in situ hybridization showed that Ccl2 is expressed by Müller cells from 12 hours of exposure, most intensely in the superior retina, in the region of the incipient light-induced lesion. After the Müller cell-driven expression of Ccl2, there was a substantial recruitment of monocytes to the local retina and choroidal vasculature. This coincided spatially with the expression of Ccl2 in the superior retina. Peak monocyte infiltration followed maximum Ccl2 expression by up to 3 days. Furthermore, Ccl2 immunoreactivity was observed in many infiltrating monocytes after a 24-hour exposure.

Conclusions. The data indicate that photoreceptor death promotes region-specific expression of Ccl2 by Müller cells, which facilitates targeting of monocytes to sites of injury. The data suggest that recruitment of monocytes to developing lesions is secondary to signaling events in the retina. (*Invest Ophthalmol Vis Sci.* 2011;52:2379–2388) DOI:10.1167/iovs.10-6010

Microglia are the principal immune cells of the central nervous system (CNS).[1] Through persistent surveillance of their microenvironment,[2] the microglia act after neuronal stress and injury, maintaining homeostasis in the CNS parenchyma, including the retina; facilitating the phagocytosis of debris and apoptotic cells,[3–5] enabling antigen presentation,[6,7] and promoting secretion of neuroprotective factors.[8] However, activated microglia may also promote the secretion of the proinflammatory mediators tumor necrosis factor (TNF)-α and interleukin (IL)-1β,[9–11] in addition to cytotoxic factors such as nitric oxide,[12–14] shown to harm neuronal cells.[12,15–18] In the retina, activated microglia respond to degeneration elicited from a range of human retinal disease, including age-related macular degeneration (AMD) (Wong JG, et al. *IOVS* 2001;42: ARVO Abstract 1222),[4,19–21] retinitis pigmentosa,[4] and late-onset retinal degeneration,[4] as well as in many experimental models of retinal degeneration.[8] In the light-induced model of photoreceptor degeneration, recruitment and activation of microglia in the retina have been particularly well characterized[22–27] and involve the infiltration of both parenchymal microglia and perivascular monocytes/microglia to the outer nuclear layer (ONL) and subretinal space after a damaging stimulus. Moreover, it has been demonstrated that attenuating the microglial response results in reduced photoreceptor death and IL1β production after light-induced damage,[26] indicating that the extensive aggregation and overactivation of microglia play a role in propagating the neurodegenerative process.

We have shown that light-induced microgliosis of perivascular monocytes is site-specific to the region of peak photoreceptor death, at the area centralis of the rat retina.[23] However, the process by which microglia are recruited into the retina after light-induced damage remains to be clarified. Chemokines have been shown to have potent chemoattractant properties in the trafficking of leukocytes in immune surveillance and inflammation in the CNS.[28–31] Chemokine expression results in the establishment of chemical ligand gradients that serve as directional cues for the guidance of certain leukocytes to sites of injury and are also thought to aid in their extravasation into tissues.[28] Studies have shown that several chemokines are expressed at high levels after light-induced damage[25,32]; the most well-characterized of these being chemokine (C-C motif) ligand 2 (Ccl2).[33] Ccl2 (also known as monocyte chemoattractant protein 1 [MCP-1]) is a strong chemoattractant for monocytes,[34,35] whose upregulation is implicated in several CNS diseases[30,31] including Alzheimer's disease,[36,37] multiple sclerosis,[38,39] and brain trauma.[40,41]

We sought to investigate the site and cellular localization of Ccl2 expression in the retina after photoreceptor death induced by exposure to bright, continuous light (BCL) and to relate this expression pattern to infiltration of perivascular monocytes/microglia (hereinafter referred to as monocytes). Our findings show that in this model, Müller cells located in the region of the incipient lesion are the early source of Ccl2, which is upregulated in concert with the onset of photoreceptor degeneration. These findings demonstrate the role of the neural retina in the active initiation of an inflammatory response, as a result of light-induced injury. This Müller cell–driven expression correlates closely with the spatial and tem-

From the [1]Research School of Biology, the [2]ARC (Australian Research Council) Centre of Excellence in Vision Science, and the [3]ANU Medical School, The Australian National University, Canberra, Australia.

Supported by Australian Research Council Centres of Excellence Program CE0561903 and an Ophthalmic Research Institute of Australia Brenda Mitchell Grant.

Submitted for publication June 7, 2010; revised September 27, 2010; accepted November 23, 2010.

Disclosure: **M. Rutar**, None; **R. Natoli**, None; **K. Valter**, None; **J.M. Provis**, None

Corresponding author: Matthew Rutar, BSB Division, RSB, Building 46, The Australian National University, Canberra ACT 0200, Australia; matt.rutar@rsbs.anu.edu.au.

poral infiltration of monocytes from both the retinal and choroidal vascular supplies, which in turn were found to express Ccl2.

METHODS

Animals and Exposure to Light

All experiments conducted were in accordance with the ARVO Statement for the Use of Animals in Ophthalmic and Vision Research. Sprague-Dawley (SD) rats were born and reared in dim cyclic light conditions with an ambient level of approximately 5 lux. The animals were exposed to BCL between postnatal day (P)130 and P160. Before BCL exposure, the animals were dark adapted for a minimum of 15 hours, then transferred to individual cages designed to allow light to enter unimpeded. BCL exposure, which was achieved with a fluorescent light source (18W, Cool White; TFC, Taipei, Taiwan) positioned above the cages, commenced daily at 9 AM and was maintained at an intensity of approximately 1000 lux at the cage floor. The animals were exposed to BCL for a period of 1, 3, 6, 12, 17, or 24 hours, after which retinal tissue was obtained for analysis. Some animals were returned to dim-light conditions immediately after 24 hours' BCL, for a period of 3 or 7 days, while postexposure effects were studied. Age-matched, dim-light–reared animals served as the controls.

Tissue Collection and Processing

Animals were euthanatized by overdose of a barbiturate administered by intraperitoneal injection (60 mg/kg bodyweight; Valabarb; Virbac, Milperra, NSW, Australia). The left eye of each animal was marked at the superior surface for orientation, enucleated, and processed for cryosectioning, and the retina of the right eye was excised through a corneal incision and prepared for RNA extraction.

Eyes for cryosectioning were immediately immersion fixed in 4% paraformaldehyde in 0.1 M PBS (pH 7.3) for 3 hours at room temperature, then washed in 0.1 M PBS before being left in a 15% sucrose solution overnight for cryoprotection. Eyes were oriented and embedded in OCT compound (Tissue-Tek; Sakura Fintek, Tokyo, Japan), snap frozen in liquid nitrogen, and cryosectioned at 16 μm. The sections were mounted on gelatin/poly-L-lysine–coated glass slides, dried overnight at 37°C, and stored at −20°C until use.

Retinas for RNA extraction were immediately deposited in RNA stabilizer (RNAlater solution, cat. no. 7024; Ambion, Austin, TX) prechilled on ice. The samples were incubated at 4°C overnight to allow adequate penetration of the preservative, and then stored at −80°C until required. The samples were processed in batches encompassing the entire time course, to ensure comparability. On extraction, the retinal samples were thawed on ice, and the RNA stabilizer was removed. RNA extraction was performed with a combination of extraction reagent (TRIzol; cat. no. 15596-026; Invitrogen, Carlsbad, CA) and a purification kit (RNAqueous-Small Scale, cat. no. 1912; Ambion) used in tandem to extract and purify the RNA respectively, as described in another publication.[42] Isolated total RNA was analyzed for quantity and purity with a spectrophotometer (ND-1000; Nanodrop Technologies, Wilmington, DE); samples with a 260/280 ratio greater than 1.90 were considered sufficient. The RNA quality in each sample was assessed with an RNA analyzer (model 2100 Bioanalyzer; Agilent Technologies, Santa Clara, CA); only samples with an integrity number (RIN) of ≥8 were used.

Quantitative Real-Time Polymerase Chain Reaction

First-strand cDNA synthesis was performed (SuperScript III Reverse Transcriptase kit, cat. no. 18080-044; Invitrogen) according to the manufacturer's instructions. A 20-μL reaction mixture was used in conjunction with 1 μg RNA, 500 ng oligo $(dT)_{18}$ primer, and 200 U reverse transcriptase. Gene amplification was measured with commercially available hydrolysis probes (TaqMan; Applied Biosystems, Inc. [ABI], Foster City, CA), the details of which are provided in Table 1. The hydrolysis probes were applied according to the manufacturer's instructions in conjunction with a master mix (Gene Expression Master-Mix, cat. no. 4369514; ABI), with the fluorescence measured on a FAM 510-nm detection channel by a qPCR system (StepOnePlus; ABI). The samples in each well were normalized by using a passive reference dye (ROX; ABI), included in the master mix, to account for well-to-well discrepancies. The amplification of each biological sample was performed in experimental duplicate, with the mean C_q (quantitation cycle) value used to determine the ratio of change in expression. The change ratio was determined by using the $\Delta\Delta C_q$ method, where the expression of the target gene was normalized relative to the expression of two reference genes, glyceraldehyde-3-phosphate dehydrogenase (GAPDH), and actin-β (Actb). Amplification specificity was assessed with gel electrophoresis.

In Situ Hybridization

To investigate the localization of Ccl2 mRNA transcripts in the retina after BCL, a riboprobe to Ccl2 was generated for in situ hybridization on retinal cryosections. Ccl2 was cloned from a PCR product (550-bp amplicon), with cDNA prepared from rat retinas (as just described), a DNA vector system (pGEM-T, cat. no. A3600; Promega, Madison, WI), and TOP10-competent cells (One Shot, cat. no. C4040-10; Invitrogen). A DIG RNA labeling kit (SP6/T7, cat. no. 1175025; Roche, Basel, Switzerland) was used to transcribe linearized plasmid and generate DIG-labeled antisense and sense riboprobes. The in situ hybridization was performed according to a protocol described elsewhere.[43] The Ccl2 riboprobe was hybridized overnight at 55°C and then washed in saline sodium citrate (pH 7.4) at 60°C.

Analysis of Cell Death

TUNEL labeling was used to quantify photoreceptor apoptosis during and after BCL, in cryosections using a protocol published previously.[44] Counts of $TUNEL^+$ cells in the ONL were performed along the full length of retinal sections cut in the parasagittal plane (superoinferior), including the optic disc, in adjacent fields measuring 1000 μm^2. The final count from each animal is the average at comparable locations in two nonsequential sections.

Immunohistochemistry

Cryosections adjacent to those used in the TUNEL analysis were used for immunohistochemistry. Details for the primary antibodies

TABLE 1. Hydrolysis Probes Used

Gene Symbol	Gene Name	Catalog No.	Entrez Gene ID
Ccl2	Chemokine (C-C motif) ligand 2	Rn01456716_g1	NM_031530.1
Gfap	Glial fibrillary acidic protein	Rn00566603_m1	NM_017009.2
GAPDH	Glyceraldehyde-3-phosphate dehydrogenase	Rn99999916_s1	NM_017008.3
Actb	Actin Beta	Rn00667869_m1	NM_031144.2

The Entrez database is provided in the public domain by the National Center for Biotechnology Information, Bethesda, MD.

TABLE 2. Antibodies

Antibody	Dilution	Source
Hamster α-Ccl2	1:100	Cat# 505902; Biolegend, San Diego, CA
Mouse α-ED1	1:200	Cat# MAB1435; Chemicon, Temecula, CA
Mouse α-S100β	1:200	Cat# 2532; Sigma-Aldrich, St. Louis, MO
Mouse α-vimentin	1:200	Cat# MAB302; Chemicon

used are shown in Table 2. After antigen retrieval (RevealIt Ag; ImmunoSolution, QLD, Australia), the sections were incubated in 10% normal goat serum (Sigma-Aldrich) for 1 hour at room temperature (RT) and incubated in the primary antibody overnight at 4°C. The sections were washed in 0.1 M PBS and incubated in the appropriate biotinylated secondary antibody for 2 hours at RT (1:200 anti-hamster IgG-biotin; Biolegend, San Diego, CA/ 1:200 biotinylated anti-mouse IgG+A+M; Invitrogen-Molecular Probes, Eugene, OR). After an additional wash in 0.1 M PBS, the sections were incubated with a streptavidin – AlexaFluor 594 conjugate (1:1000; Invitrogen-Molecular Probes) for 1.5 hours at RT. To block autofluorescence, we performed an incubation using 0.05% Sudan Black B, as described elsewhere.[45] Sections were then stained (either 1:1000 bis benzamide; Calbiochem, La Jolla, CA, or 1:1000 Syto12; Invitrogen-Molecular Probes), to visualize the cellular layers, and coverslipped with aqueous mounting medium (Aquamount, cat. no. 18606; Polysciences, Warrington, PA). Primary antibodies were omitted to control for nonspecific binding of the secondary antibody. Immunofluorescence was viewed with a laser scanning microscope (Carl Zeiss Meditec, Dublin CA) and acquired with Pascal software (ver. 4.0, Carl Zeiss Meditec). Images were enhanced for publication with image-management software (Photoshop; Adobe systems, Mountain View, CA), which was standardized between images.

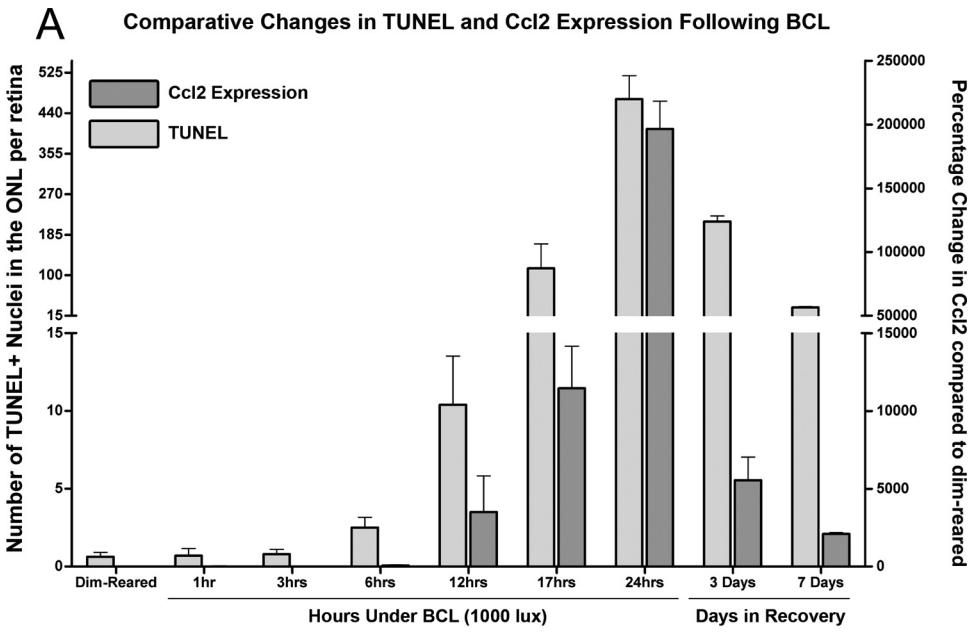

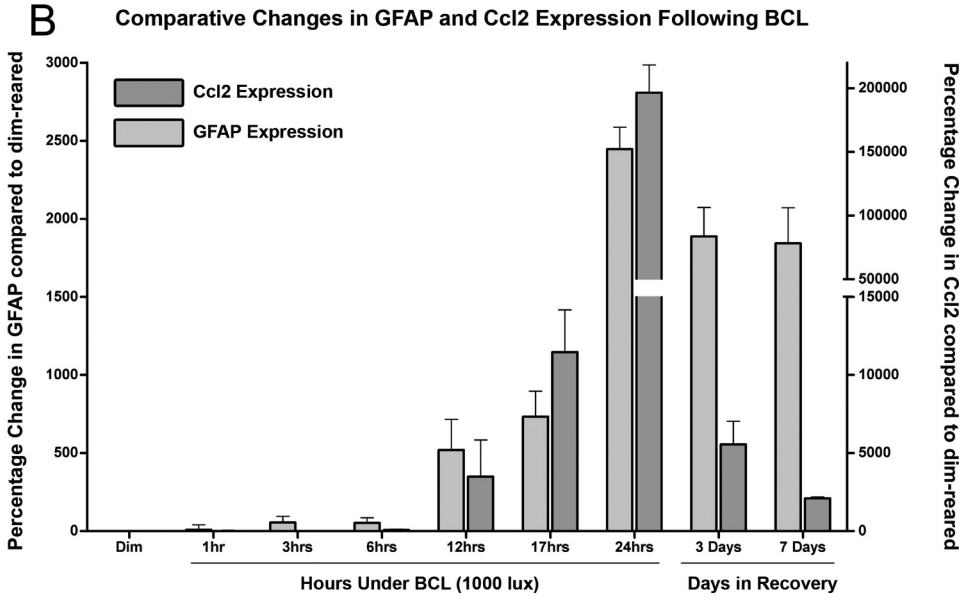

FIGURE 1. Expression of Ccl2 in the neural retina by qPCR in relation to (**A**) photoreceptor cell death and (**B**) GFAP expression, after exposure to BCL. (**A**, **B**) At 12 hours, exposure to BCL induced a significant increase in the expression of Ccl2 relative to dim-light–reared animals ($P < 0.0001$, one-way ANOVA). Ccl2 expression continued to rise significantly, reaching a peak differential expression of 196,479% by 24 hours. Seven days after exposure, relative expression had fallen sharply to 2092%. Large increases in $TUNEL^+$ nuclei in the ONL (**A**) and GFAP expression (**B**) were also observed after 12 hours of exposure ($P < 0.0001$, one-way ANOVA), correlating with the rapid upregulation of Ccl2 expression over the same period (interaction 43.60% and 42.82% of total variance, respectively, $P < 0.0001$; two-way ANOVA). (Ccl2 qPCR, $n = 4$; GFAP qPCR, $n = 4$; TUNEL, $n = 5$ per time point; error bars, SEM).

Monocyte Quantification

Monocyte counts were performed on sections immunolabeled with ED-1, a marker for perivascular monocytes/microglia,[46] and bis benzamide (as per the methodology described earlier). Counts of ED1-positive nuclei performed along the full length of retinal sections cut in the parasagittal plane (superoinferior), including the optic disc, in adjacent fields measuring 1000 μm^2. The number of monocytes in the superficial vasculature, deep vasculature, ONL, and choroidal vasculature were assessed, where the graphs showing the number of ED-1-positive cells include the total number in each field of view.

Statistical Analysis

Statistical analysis was performed with the one-way ANOVA, two-way ANOVA, or the unpaired Student's *t*-test. For each analysis, differences with a $P < 0.05$ were considered statistically significant. The one-way ANOVA, and unpaired Student's *t*-test were used for the quantification of TUNEL and monocytes, whereas qPCR results were analyzed by both the one- and the two-way ANOVA.

Results

Time Course of TUNEL Labeling and GFAP and Ccl2 Expression

During the first 12 hours of exposure to BCL the average number of $TUNEL^+$ photoreceptors increased from near 0 to 10 ($P < 0.05$, Student's *t*-test) and reached a peak of 470 by 24 hours of exposure ($P < 0.0001$, Student's *t*-test). During the postexposure period, the number of $TUNEL^+$ nuclei decreased to 213 by 3 days and then to 33 after 7 days ($P < 0.01$, Student's *t*-test). Using qPCR, we also detected modulation of GFAP expression over the experimental period ($P < 0.0001$, one-way ANOVA). GFAP expression reached peak levels at 24 hours (2446% relative to control levels) and was somewhat reduced by 7 days after exposure. These data are shown in Figure 1, where the expression levels of Ccl2 are plotted alongside both the time course of photoreceptor death (TUNEL; Fig. 1A) and expression levels of GFAP (Fig. 1B).

Exposure to BCL induced a significant differential expression of retinal Ccl2 mRNA relative to dim-light–reared animals over the experimental period ($P < 0.0001$; one-way ANOVA; Figs. 1A, 1B). By 12 hours of exposure, qPCR showed a 3499% increase in Ccl2 expression relative to dim-light–reared controls. Levels of Ccl2 mRNA reached a peak of 196,479% at 24 hours. In the postexposure period, Ccl2 expression fell to 5547% of control levels by 3 days and to 2092% by 7 days after exposure. The progressive increase in Ccl2 expression observed in the 24 hours of the exposure period correlated significantly with TUNEL labeling over the same period (interaction 43.60% of total variance; $P < 0.0001$, two-way ANOVA; Fig. 1A). Expression of GFAP and Ccl2 also correlated significantly in the 24-hour exposure period (interaction 42.82% of total variance; $P < 0.0001$, two-way ANOVA; Fig. 1B). However, GFAP expression in the recovery period did not show a clear downward trend, in contrast to a progressive reduction in expression of Ccl2 after exposure.

Localization of Ccl2 Expression

Ccl2 mRNA was not detectable by in situ hybridization in retinas of dim-light–reared animals (Fig. 2A). However, in experimental animals at 12 hours of exposure, we detected the expression of Ccl2 mRNA in isolated cells within the inner nuclear layer (INL) of the superior retina (Fig. 2B); by 24 hours BCL, we detected robust expression of Ccl2 in many cells and

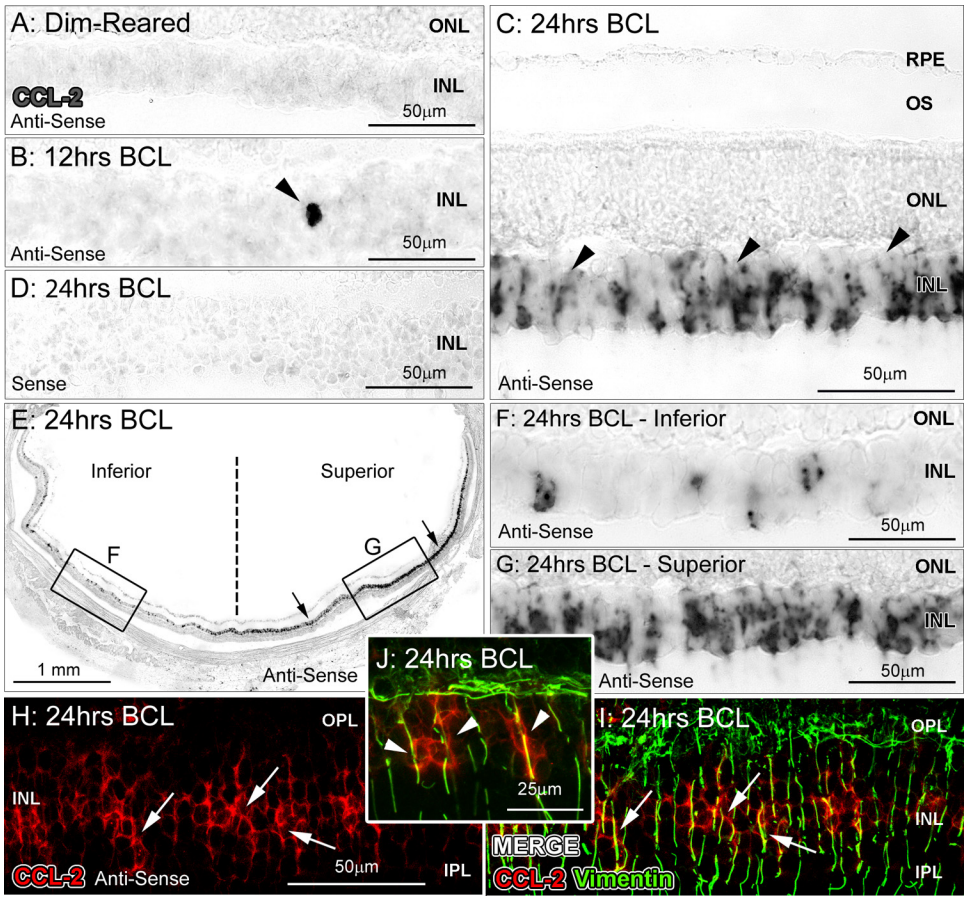

Figure 2. In situ hybridization for Ccl2 mRNA after exposure to BCL. (**A**) Expression of Ccl2 was not detectable in retinas from control, dim-light–reared animals. (**B**) Ccl2 mRNA expression was detected in isolated cells of the INL in the superior retina by 12 hours of BCL (*arrowhead*). (**C**) After exposure to 24 hours of BCL, Ccl2 mRNA was observed in cells with radially oriented processes throughout the INL (*arrowheads*). (**D**) Staining was not observed with the sense Ccl2 riboprobe in retinas after 24 hours of BCL. (**E–G**) The distribution of Ccl2 expression was detected in a superoinferior gradient, after BCL, with the most intense labeling detected in the superior retina. (**H–J**) Ccl2 expression (*red*, *arrows*) in sections counterimmunolabeled with anti-vimentin, showing double-labeled Müller cell processes (*green*; *arrows*, *arrowheads*) indicating that Ccl2 in the INL is expressed by Müller cells. INL, inner nuclear layer; IPL, inner plexiform layer; ONL, outer nuclear layer; OPL, outer plexiform layer; RPE, retinal pigment epithelium.

processes in the INL (Fig. 2C), consistent with the qPCR expression profile (Fig. 1). We also observed that Ccl2 expression was distributed in a superoinferior gradient after BCL, with peak expression observed within the superior midperiphery (Figs. 2E–G). The fluorescent markers showed that the Ccl2 mRNA (Figs. 2H–J; arrows) co-localized with the vimentin-immunoreactive Müller cell processes (Figs. 2H–J; arrows), suggesting that Ccl2 is initially expressed by the Müller cells.

There was no immunoreactivity (IR) for Ccl2 protein in dim-light–reared animals (Fig. 3A), but in experimental animals at 12 hours of exposure, some Ccl2-IR was present in radially oriented processes in the superior retina (Figs. 3B, 3C) and in an increasing number of processes at 24 hours of exposure (Fig. 3D). Double immunolabeling with the Müller-cell–specific protein S100β (Figs. 3I–K) showed Ccl2-IR localized within the inner processes of Müller cells, consistent with the in situ hybridization results (Fig. 2). Ccl2-IR Müller cell processes were most prominent at 24 hours of BCL exposure (Fig. 3D) and declined markedly in the postexposure period (Figs. 3E, 3F), so that relatively few Ccl2-IR processes were present by 7 days after exposure (Fig. 3F). As with the distribution of Ccl2 mRNA (Fig. 2E), Ccl2-IR was predominant in Müller cell processes in the superior retina after exposure to BCL (Figs. 3G, 3H).

Quantification of ED-1-Positive Monocytes

The histograms in Figure 4 show the number of monocytes in the retina and choroid. The total number of monocytes in the retina and choroid remained unchanged in the first 17 hours of BCL exposure, but increased significantly by 24 hours of exposure, compared with the dim-light–reared controls ($P < 0.01$, Student's *t*-test; Fig. 4A). Peak numbers of monocytes were detected at 3 days after exposure (196 cells; $P < 0.05$, Student's *t*-test), which were significantly diminished by 7 days (123 cells; $P < 0.05$, Student's *t*-test). The overall trend in monocyte infiltration was found to be highly significant by one-way ANOVA ($P < 0.0001$). The counts of recruited cells in different locations (retinal vasculature, choroid, and ONL) are shown in Figure 4B. The data show significant monocyte recruitment after BCL in both the choroid and retinal vasculature, reaching peak numbers in the retinal vasculature by 24 hours of exposure and in the choroid at 3 days ($P < 0.001$, one-way ANOVA). The peak number of monocytes was also detected in the ONL by 3 days ($P < 0.01$, one-way ANOVA). While a larger number of ED-1$^+$ cells were detected in the choroid (compared with the count in the retinal vessels), the data indicate that recruitment of monocytes from the retinal vessels occurred earlier than the from the choroid, with the number of cells rising acutely from a baseline of near 0 to 16 cells per retina, between 12 and 17 hours of BCL exposure ($P < 0.01$, Student's *t*-test).

The distribution of the infiltrating monocytes along the vertical axis of the retina is shown in Figure 5. In dim-light–reared animals, circulating monocytes were evenly distributed across the superior and inferior retina (Fig. 5A). By 24 hours of BCL exposure, the monocytes were more numerous in the superior retina by a ratio of approximately 2:1 ($P < 0.05$, Student's *t*-test; Fig. 5A). By 3 days, there were more than six times as many monocytes in the superior retina than in the inferior retina, and the number remained elevated in the superior retina at 7 days after exposure ($P < 0.01$, Student's *t*-test). A more detailed analysis of the distribution of monocytes in adjacent fields along the vertical axis of the retina, at different times of BCL exposure and recovery, is shown in Figure 5B. The data indicate that monocyte numbers reached a peak at 3 days after exposure, in the region of the superior retina that corresponds to the incipient "hot-spot" of degeneration, characterized in our previous investigation.[23]

We also found that many infiltrating monocytes in the superior retina expressed Ccl2 after exposure to BCL (Fig. 6). After 24 hours of BCL, many infiltrating monocytes within the choroid were Ccl2-IR (Fig. 6A–C). Extravasated tissue macro-

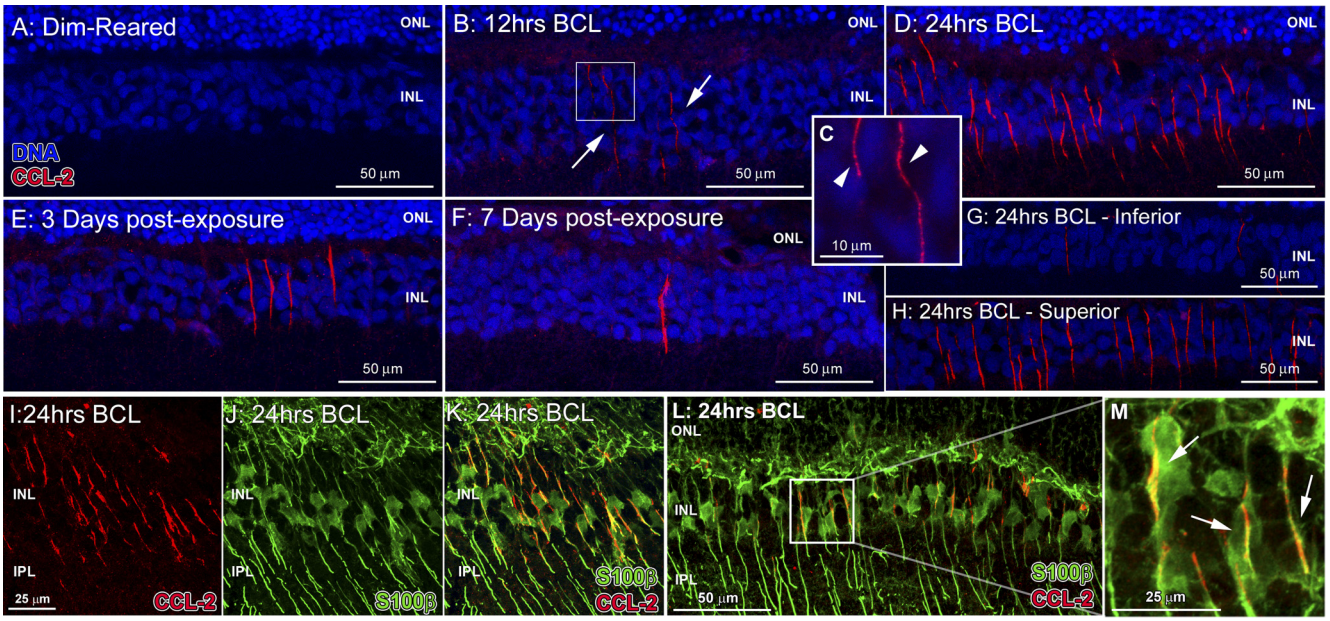

Figure 3. IR for Ccl2 in Müller cells after exposure to BCL. (**A**) IR for Ccl2 was not detected in control dim-light–reared retinas. (**B**, **C**) Faint Ccl2-IR (*red*, *arrows*) was detected in thin, radial processes (*arrowheads*) in the INL of the superior retina at 12 hours of BCL exposure. (**D**) By 24 hours of BCL exposure, Ccl2-IR was present in a large number of radial processes in the superior retina. (**E**, **F**) Lower levels of Ccl2-IR were evident during the postexposure period. (**G**, **H**) Ccl2-IR processes were more numerous in the superior (**H**) compared with the inferior (**G**) retina. (**I**–**M**) Dual immunolabeling for Ccl2 (*red*) and the Müller-cell-specific protein S100β (*green*) shows the co-localization of Ccl2 IR with S100β (**K**) in Müller cell processes. (**L**) Field with *inset* showing co-localization of Ccl2 and S100β-IR (**M**) in the inner processes of Müller cells (*arrows*). INL, inner nuclear layer; IPL, inner plexiform layer; ONL, outer nuclear layer.

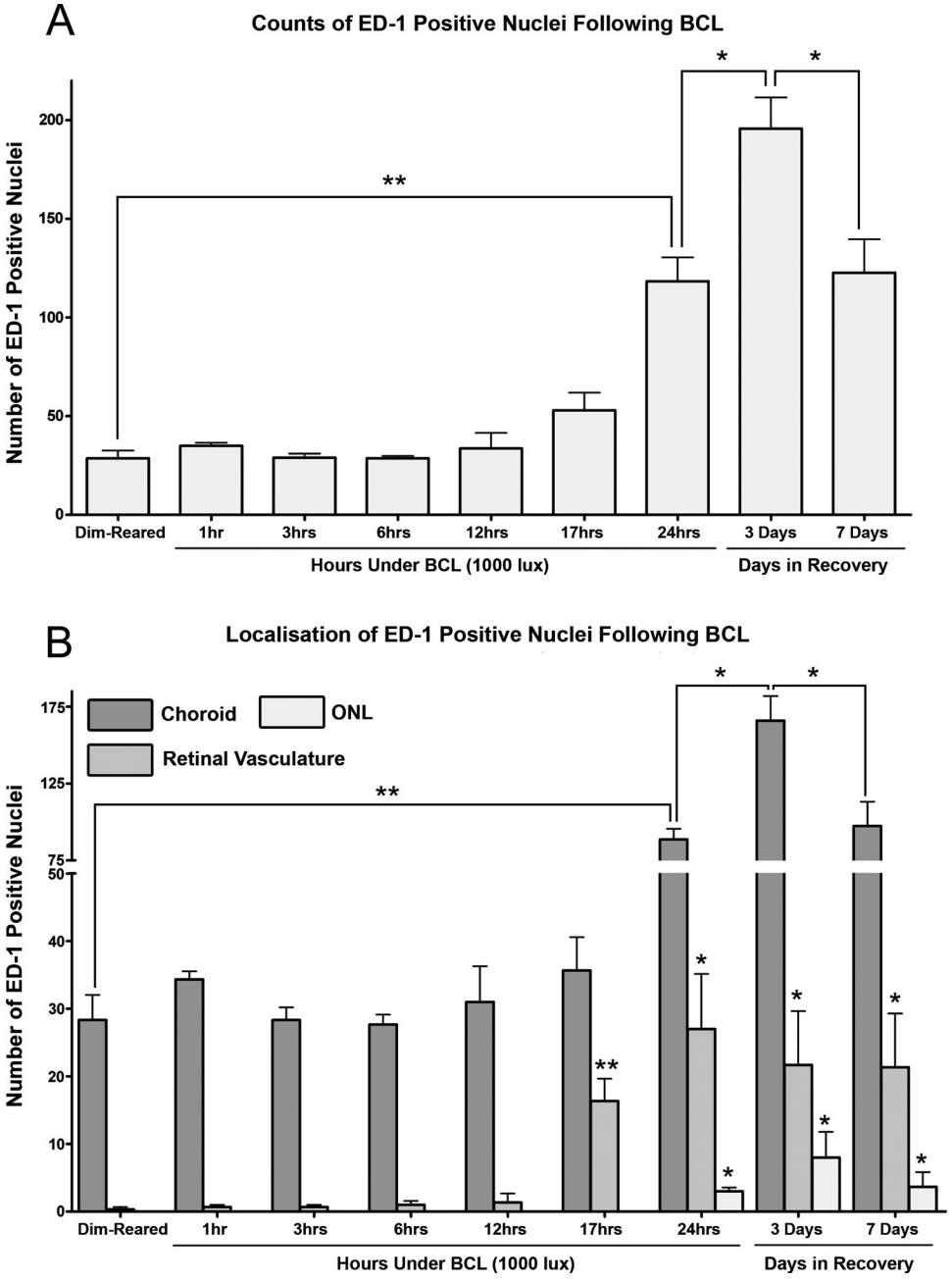

FIGURE 4. Recruitment of monocytes from the choroid and neural retina after BCL. (**A**) Increased number of monocytes are detected in the retina and choroid between 12 and 24 hours of exposure; monocytes continued to accumulate in the retina and choroid after exposure, reaching a peak at 3 days ($P < 0.001$, one-way ANOVA). (**B**) After the onset of BCL exposure, significant monocyte recruitment was observed in all locations of the tissue examined, including the retinal vasculature, choroid, and ONL ($P < 0.05$, one-way ANOVA; $n = 3$ per time point; error bars represent SEM; *Asterisks* denote significant change according to Student's *t*-test, versus dim-light–reared animals unless otherwise noted, where $^{*}P < 0.05$ and $^{**}P < 0.01$).

phages located within the outer segment layer (Fig. 6A) and the ONL (Fig. 6D) were also strongly Ccl2-IR. $Ccl2^{+}$ monocytes were observed predominately at 24 hours of BCL exposure; none were observed in the early exposure period (12 hours BCL), coinciding with the emergence of Ccl2 expression by Müller cells. By the postexposure period, relatively few Ccl2-IR monocytes were detected (data not shown).

DISCUSSION

The results of this study confirm the early and robust upregulation of Ccl2 in conjunction with the light-mediated induction of photoreceptor death and the expression of the stress-factor GFAP, consistent with findings from previous studies.[25,32] Our data also elaborate on the role of Ccl2 in light-mediated retinal dystrophy, through several key findings. First, both in situ hybridization and immunohistochemistry verified that Ccl2 was expressed early by the Müller glia after exposure to BCL, whose expression—predominately in the superior retina—was consistent with both the temporal and spatial onset of photoreceptor apoptosis.[23,47] Second, a preferential recruitment of monocytes to both retinal and choroidal vascular supplies occurred in the superior retinal after the expression of Ccl2, which correlates with the spatial distribution of Ccl2-positive Müller cells. Third, our data show that extravasating monocytes provided additional stimulatory expression of Ccl2 after 24 hours of BCL after the initial expression driven by the Müller cells.

Although the expression of Ccl2 in light-damaged retinas has been documented previously through PCR,[32] the precise distribution and cellular localization of Ccl2 expression after the damaging stimulus has not, to our knowledge, been investigated. Zhang et al.[25] hypothesized that Müller cells or retinal pigment epithelial cells (RPE) may be the source of chemo-

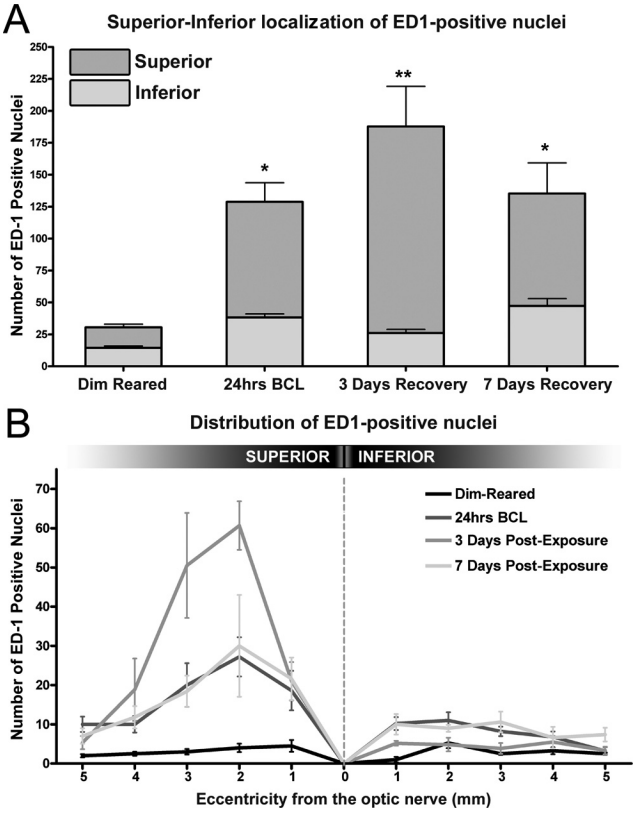

FIGURE 5. Distribution of monocyte recruitment in relation to the expression and IR for Ccl2 after BCL exposure. (**A**) The total number of monocytes in superior and inferior regions of the retina. There was a significant preferential recruitment of monocytes in the superior retina after 24 hours BCL that persisted to the postexposure time points. (**B**) The distribution of monocytes across the vertical meridian of the retina. At 24 hours BCL and 3 and 7 days after exposure, monocytes were recruited primarily into the superior retina and were concentrated in a region approximately 2 mm superior to the optic nerve ($n = 4$ per time point; error bars, SEM; *Asterisks* denote a significant change according to Student's *t*-test, compared to the inferior retina, $^{*}P < 0.05$ and $^{**}P < 0.01$).

kines after BCL, and several in vitro studies have shown that RPE cell cultures express Ccl2,[48] including in response to the introduction of stimulatory cytokines.[49–53] This investigation, however, is the first to show the preferential distribution of Ccl2 mRNA in Müller cells in the region of the incipient lesion, with as little as 12 hours of exposure to BCL. The findings pinpoint a response by Müller cells—not RPE cells—as the primary source of local Ccl2 expression, which promotes the monocyte infiltration that is associated with light-mediated photoreceptor apoptosis. The present findings are consistent with those in a previous study of experimental retinal detachment, which showed a rapid upregulation of Ccl2 expression in microdissected sections of the INL and the localization of Ccl2-IR in Müller cells that correlated with detachment-induced photoreceptor death.[54]

Our data also demonstrate an important role for chemokines in mediating local neuroinflammatory responses driven by the neural retina. Ccl2 is a potent chemokine for monocytes in vitro[35] and is induced in a range of CNS diseases.[30] Its rapid site-specific expression by Müller cells, as demonstrated in the present study, appears to serve as an early proinflammatory signal that targets monocytes to sites of degeneration. We propose that Ccl2 expression is stimulated in Müller cells as a result of regional photoreceptor apoptosis, since increased levels of apoptotic photoreceptors are detected around 6 hours before increased levels of Ccl2 are detected (Fig. 1A). After Ccl2 upregulation, our data also showed preferential infiltration of monocytes from retinal and choroidal vascular supplies into the superior retina, consistent with our previous findings[23] and correlating with the spatial distribution of $Ccl2^{+}$ Müller cells.

Perivascular monocytes express the Ccr2 chemokine receptor, of which Ccl2 is a known ligand,[55] and $ED\text{-}1^{+}$ monocytes specifically have been shown to express Ccr2.[56] Our findings are consistent with those in previous investigations that have established Ccl2 as a key factor in the chemotactic guidance of monocytes after injury. An investigation in experimental retinal detachment in Ccl2-deficient knockout mice and Ccl2-specific antibody neutralization showed a substantial decrease in monocyte recruitment after detachment in conjunction with reduced photoreceptor death compared with the controls.[57] Similar deficiencies in monocyte recruitment have also been reported after Ccl2 inhibition in a variety of models, including skin inflammation,[58] thioglycollate challenge,[59] experimental autoimmune encephalomyelitis,[60] pulmonary granuloma,[59] and peripheral endotoxin insult.[61] Despite these findings, however, in a recent study, Joly et al.[62] did not observe a difference in the population of F4/80-positive macrophages in the subretinal space after light-induced damage in Ccl2-knockout mice. However, those authors did not assess the expression of other microglial markers, such as ED-1, nor did they determine whether the $F4/80^{+}$ cells expressed the Ccr2 receptor. Indeed, a study in lung infection showed that <10% of $F4/80^{bright}$ cells express Ccr2, suggesting that they are resident, rather than recruited, macrophages.[63]

Our findings also show that many extravasating monocytes in the superior retina display strong IR for Ccl2 after 24 hours of BCL, contributing to the vast increase in Ccl2 mRNA observed by qPCR at 24 hours of BCL. Such expression is consistent with the altered responsiveness in monocytes as they differentiate to form tissue macrophages, resulting in a concomitant downregulation of the Ccr2 receptor and an enhancement of Ccl2 secretion after endothelial adherence.[64] This modulation of Ccr2 may act as a regulatory mechanism for controlling the extent of macrophage activation,[64] whereas the upregulation of Ccl2 could serve to refine and amplify the Ccl2 gradient initially laid forth by the Müller cells.

Relevance to AMD

Our previous findings, in conjunction with those in other studies, suggest that the light-mediated model of retinal degeneration has several features in common with the pathogenesis of AMD.[23,65,66] This model, like the established laser-induced model of neovascular AMD, uses an acute damaging stimulus to evoke long-term, site-specific retinal degeneration. We have recently shown recruitment of monocytes/macrophages to incipient lesion on the visual axis (area centralis) of the rat retina after BCL injury.[23] Activated macrophages are associated with the progression and severity of AMD,[67] and several studies show that macrophage/microglial inhibition reduce lesion size in the laser-induced model of neovascular AMD.[68–70] The light-induced damage model used in this study involved localized macrophage recruitment to the site of retinal damage[23] and endogenous Ccl2 expression in the neural retina (present study). These findings provide insight into the mechanisms that guide macrophages to regions of incipient degeneration, which may be common to AMD.

Although direct studies of Ccl2 expression in the human retina are lacking,[71] it has been shown that both Ccl2- and Ccr2-knockout mice exhibit reduced lesion size and macro-

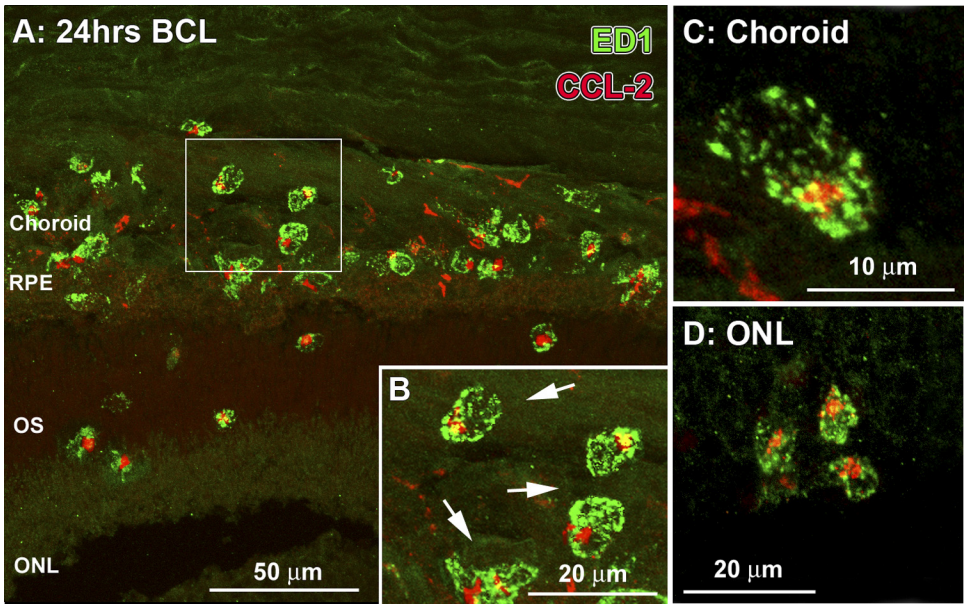

FIGURE 6. Ccl2-IR (*red*) and ED-1-IR (*green*) monocytes at 24 hours BCL. (**A**, **B**) Many infiltrating ED-1-positive nuclei were also Ccl2-IR, in the choroid and retina. (**C**) An extravasated monocyte in the choroid, double labeled for Ccl2 and ED-1. (**D**) A cluster of extravasated Ccl2 and ED-1-IR monocytes in the ONL. ONL, outer nuclear layer; OS, outer segments; RPE, retinal pigment epithelium.

phage infiltration after laser-induced choroidal neovascularization compared with controls.[72,73] It has been suggested that aging Ccl2/Ccr2-knockout mice develop AMD-like retinal degeneration,[74] indicating that Ccl2 is also necessary for retinal homeostasis, although the AMD-like phenotype in the knockout has been questioned recently.[72] Despite this, the findings suggest a role for Ccl2-induced monocyte trafficking in the pathogenesis of AMD, and point to a possible role of the retina in localization of the lesions to the macula.

CONCLUSION

While the recruitment of microglia has been thought to serve a beneficial function after retinal injury, such as promoting the removal of cellular debris and apoptotic cells,[5] recent evidence has suggested that the extensive microglial activation induced in BCL is detrimental.[26] Our data demonstrate that monocyte recruitment after light-mediated cell death correlates with both the temporal and spatial expression of Ccl2 by Müller cells, which supports a role of the neural retina in guiding neuroinflammatory responses of microglia after damage. The potential modulation of such endogenous chemokine responses may provide a powerful means of controlling excessive microglial recruitment and activation, which has relevance in the treatment of human diseases such as AMD.

References

1. Davoust N, Vuaillat C, Androdias G, Nataf S. From bone marrow to microglia: barriers and avenues. *Trends Immunol.* 2008;29:227–234.
2. Nimmerjahn A, Kirchhoff F, Helmchen F. Resting microglial cells are highly dynamic surveillants of brain parenchyma in vivo. *Science.* 2005;308:1314–1318.
3. Bauer J, Sminia T, Wouterlood FG, Dijkstra CD. Phagocytic activity of macrophages and microglial cells during the course of acute and chronic relapsing experimental autoimmune encephalomyelitis. *J Neurosci Res.* 1994;38:365–375.
4. Gupta N, Brown KE, Milam AH. Activated microglia in human retinitis pigmentosa, late-onset retinal degeneration, and age-related macular degeneration. *Exp Eye Res.* 2003;76:463–471.
5. Neumann H, Kotter MR, Franklin RJ. Debris clearance by microglia: an essential link between degeneration and regeneration. *Brain.* 2009;132:288–295.
6. Penfold PL, Liew SC, Madigan MC, Provis JM. Modulation of major histocompatibility complex class II expression in retinas with age-related macular degeneration. *Invest Ophthalmol Vis Sci.* 1997;38:2125–2133.
7. Penfold PL, Provis JM, Liew SC. Human retinal microglia express phenotypic characteristics in common with dendritic antigen-presenting cells. *J Neuroimmunol.* 1993;45:183–191.
8. Langmann T. Microglia activation in retinal degeneration. *J Leukoc Biol.* 2007;81:1345–1351.
9. Sawada M, Kondo N, Suzumura A, Marunouchi T. Production of tumor necrosis factor-alpha by microglia and astrocytes in culture. *Brain Res.* 1989;491:394–397.
10. Kim SU, de Vellis J. Microglia in health and disease. *J Neurosci Res.* 2005;81:302–313.
11. Hanisch UK. Microglia as a source and target of cytokines. *Glia.* 2002;140–155.
12. Boje KM, Arora PK. Microglial-produced nitric oxide and reactive nitrogen oxides mediate neuronal cell death. *Brain Res.* 1992;587:250–256.
13. Ding AH, Nathan CF, Stuehr DJ. Release of reactive nitrogen intermediates and reactive oxygen intermediates from mouse peritoneal macrophages: comparison of activating cytokines and evidence for independent production. *J Immunol.* 1988;141:2407–2412.
14. Garden GA, Moller T. Microglia biology in health and disease. *J Neuroimmune Pharmacol.* 2006;1:127–137.
15. Yang LP, Zhu XA, Tso MO. A possible mechanism of microglia-photoreceptor crosstalk. *Mol Vis.* 2007;13:2048–2057.
16. Roque RS, Rosales AA, Jingjing L, Agarwal N, Al-Ubaidi MR. Retina-derived microglial cells induce photoreceptor cell death in vitro. *Brain Res.* 1999;836:110–119.
17. Chao CC, Hu S, Ehrlich L, Peterson PK. Interleukin-1 and tumor necrosis factor-alpha synergistically mediate neurotoxicity: involvement of nitric oxide and of N-methyl-D-aspartate receptors. *Brain Behav Immun.* 1995;9:355–365.
18. McGuire SO, Ling ZD, Lipton JW, Sortwell CE, Collier TJ, Carvey PM. Tumor necrosis factor alpha is toxic to embryonic mesencephalic dopamine neurons. *Exp Neurol.* 2001;169:219–230.
19. Ezzat MK, Hann CR, Vuk-Pavlovic S, Pulido JS. Immune cells in the human choroid. *Br J Ophthalmol.* 2008;92:976–980.
20. Penfold PL, Killingsworth MC, Sarks SH. Senile macular degeneration. The involvement of giant cells in atrophy of the retinal pigment epithelium. *Invest Ophthalmol Vis Sci.* 1986;27:364–371.
21. Cherepanoff S, McMenamin PG, Gillies MC, Kettle E, Sarks SH. Bruch's membrane and choroidal macrophages in early and ad-

vanced age-related macular degeneration. *Br J Ophthalmol.* 2010; 94:918–925.

22. Ng TF, Streilein JW. Light-induced migration of retinal microglia into the subretinal space. *Invest Ophthalmol Vis Sci.* 2001;42: 3301–3310.
23. Rutar M, Provis J, Valter K. Brief exposure to damaging light causes focal recruitment of macrophages, and long-term destabilization of photoreceptors in the albino rat retina. *Curr Eye Res.* 2010;35: 631–643.
24. Gordon WC, Casey DM, Lukiw WJ, Bazon NG. DNA damage and repair in light-induced photoreceptor degeneration. *Invest Ophthalmol Vis Sci.* 2002;43:3511–3521.
25. Zhang C, Shen JK, Lam TT, et al. Activation of microglia and chemokines in light-induced retinal degeneration. *Mol Vis.* 2005; 11:887–895.
26. Ni YQ, Xu GZ, Hu WZ, Shi L, Qin YW, Da CD. Neuroprotective effects of naloxone against light-induced photoreceptor degeneration through inhibiting retinal microglial activation. *Invest Ophthalmol Vis Sci.* 2008;49:2589–2598.
27. Santos AM, Martin-Oliva D, Ferrer-Martin RM, et al. Microglial response to light-induced photoreceptor degeneration in the mouse retina. *J Comp Neurol.* 2010;518:477–492.
28. Luster AD. Chemokines: chemotactic cytokines that mediate inflammation. *N Engl J Med.* 1998;338:436–445.
29. Oppenheim JJ, Zachariae CO, Mukaida N, Matsushima K. Properties of the novel proinflammatory supergene "intercrine" cytokine family. *Annu Rev Immunol.* 1991;9:617–648.
30. Bajetto A, Bonavia R, Barbero S, Schettini G. Characterization of chemokines and their receptors in the central nervous system: physiopathological implications. *J Neurochem.* 2002;82:1311–1329.
31. Ransohoff RM, Glabinski A, Tani M. Chemokines in immune-mediated inflammation of the central nervous system. *Cytokine Growth Factor Rev.* 1996;7:35–46.
32. Chen L, Wu W, Dentchev T, et al. Light damage induced changes in mouse retinal gene expression. *Exp Eye Res.* 2004;79:239–247.
33. Deshmane SL, Kremlev S, Amini S, Sawaya BE. Monocyte chemoattractant protein-1 (MCP-1): an overview. *J Interferon Cytokine Res.* 2009;29:313–326.
34. Matsushima K, Larsen CG, DuBois GC, Oppenheim JJ. Purification and characterization of a novel monocyte chemotactic and activating factor produced by a human myelomonocytic cell line. *J Exp Med.* 1989;169:1485–1490.
35. Yoshimura T, Robinson EA, Tanaka S, Appella E, Kuratsu J, Leonard EJ. Purification and amino acid analysis of two human glioma-derived monocyte chemoattractants. *J Exp Med.* 1989;169:1449–1459.
36. Prat E, Baron P, Meda L, et al. The human astrocytoma cell line U373MG produces monocyte chemotactic protein (MCP)-1 upon stimulation with beta-amyloid protein. *Neurosci Lett.* 2000;283: 177–180.
37. Johnstone M, Gearing AJ, Miller KM. A central role for astrocytes in the inflammatory response to beta-amyloid; chemokines, cytokines and reactive oxygen species are produced. *J Neuroimmunol.* 1999;93:182–193.
38. Simpson JE, Newcombe J, Cuzner ML, Woodroofe MN. Expression of monocyte chemoattractant protein-1 and other beta-chemokines by resident glia and inflammatory cells in multiple sclerosis lesions. *J Neuroimmunol.* 1998;84:238–249.
39. McManus C, Berman JW, Brett FM, Staunton H, Farrell M, Brosnan CF. MCP-1, MCP-2 and MCP-3 expression in multiple sclerosis lesions: an immunohistochemical and in situ hybridization study. *J Neuroimmunol.* 1998;86:20–29.
40. Glabinski AR, Balasingam V, Tani M, et al. Chemokine monocyte chemoattractant protein-1 is expressed by astrocytes after mechanical injury to the brain. *J Immunol.* 1996;156:4363–4368.
41. Muessel MJ, Berman NE, Klein RM. Early and specific expression of monocyte chemoattractant protein-1 in the thalamus induced by cortical injury. *Brain Res.* 2000;870:211–221.
42. Natoli R, Provis J, Valter K, Stone J. Gene regulation induced in the C57BL/6J mouse retina by hyperoxia: a temporal microarray study. *Mol Vis.* 2008;14:1983–1994.
43. Cornish EE, Madigan MC, Natoli R, Hales A, Hendrickson AE, Provis JM. Gradients of cone differentiation and FGF expression during development of the foveal depression in macaque retina. *Vis Neurosci.* 2005;22:447–459.
44. Maslim J, Valter K, Egensperger R, et al. Tissue oxygen during a critical developmental period controls the death and survival of photoreceptors. *Invest Ophthalmol Vis Sci.* 1997;38:1667–1677.
45. Schnell SA, Staines WA, Wessendorf MW. Reduction of lipofuscin-like autofluorescence in fluorescently labeled tissue. *J Histochem Cytochem.* 1999;47:719–730.
46. Chen L, Yang P, Kijlsta A. Distribution, markers, and functions of retinal microglia. *Occul Immunol Inflamm.* 2002;10:27–39.
47. Tanito M, Kaidzu S, Ohira A, Anderson RE. Topography of retinal light damage in light-exposed albino rats. *Exp Eye Res.* 2008;87: 292–295.
48. Elner SG, Strieter RM, Elner VM, Rollins BJ, Del Monte MA, Kunkel SL. Monocyte chemotactic protein gene expression by cytokine-treated human retinal pigment epithelial cells. *Lab Invest.* 1991; 64:819–825.
49. Shi G, Maminishkis A, Banzon T, et al. Control of chemokine gradients by the retinal pigment epithelium. *Invest Ophthalmol Vis Sci.* 2008;49:4620–4630.
50. Elner SG, Elner VM, Bian ZM, et al. Human retinal pigment epithelial cell interleukin-8 and monocyte chemotactic protein-1 modulation by T-lymphocyte products. *Invest Ophthalmol Vis Sci.* 1997; 38:446–455.
51. Elner VM, Burnstine MA, Strieter RM, Kunkel SL, Elner SG. Cell-associated human retinal pigment epithelium interleukin-8 and monocyte chemotactic protein-1: immunochemical and in-situ hybridization analyses. *Exp Eye Res.* 1997;65:781–789.
52. Bian ZM, Elner SG, Strieter RM, Kunkel SL, Lukacs NW, Elner VM. IL-4 potentiates IL-1beta- and TNF-alpha-stimulated IL-8 and MCP-1 protein production in human retinal pigment epithelial cells. *Curr Eye Res.* 1999;18:349–357.
53. Holtkamp GM, Kijlstra A, Peek R, de Vos AF. Retinal pigment epithelium-immune system interactions: cytokine production and cytokine-induced changes. *Prog Retin Eye Res.* 2001;20:29–48.
54. Nakazawa T, Matsubara A, Noda K, et al. Characterization of cytokine responses to retinal detachment in rats. *Mol Vis.* 2006; 12:867–878.
55. Yoshimura T, Leonard EJ. Identification of high affinity receptors for human monocyte chemoattractant protein-1 on human monocytes. *J Immunol.* 1990;145:292–297.
56. Guazzone VA, Rival C, Denduchis B, Lustig L. Monocyte chemoattractant protein-1 (MCP-1/CCL2) in experimental autoimmune orchitis. *J Reprod Immunol.* 2003;60:143–157.
57. Nakazawa T, Hisatomi T, Nakazawa C, et al. Monocyte chemoattractant protein 1 mediates retinal detachment-induced photoreceptor apoptosis. *Proc Natl Acad Sci U S A.* 2007;104:2425–2430.
58. Palframan RT, Jung S, Cheng G, et al. Inflammatory chemokine transport and presentation in HEV: a remote control mechanism for monocyte recruitment to lymph nodes in inflamed tissues. *J Exp Med.* 2001;194:1361–1373.
59. Lu B, Rutledge BJ, Gu L, et al. Abnormalities in monocyte recruitment and cytokine expression in monocyte chemoattractant protein 1-deficient mice. *J Exp Med.* 1998;187:601–608.
60. Huang DR, Wang J, Kivisakk P, Rollins BJ, Ransohoff RM. Absence of monocyte chemoattractant protein 1 in mice leads to decreased local macrophage recruitment and antigen-specific T helper cell type 1 immune response in experimental autoimmune encephalomyelitis. *J Exp Med.* 2001;193:713–726.
61. Thompson WL, Karpus WJ, Van Eldik LJ. MCP-1-deficient mice show reduced neuroinflammatory responses and increased peripheral inflammatory responses to peripheral endotoxin insult. *J Neuroinflammation.* 2008;5:35.
62. Joly S, Samardzija M, Wenzel A, Thiersch M, Grimm C. Nonessential role of beta3 and beta5 integrin subunits for efficient clearance of cellular debris after light-induced photoreceptor degeneration. *Invest Ophthalmol Vis Sci.* 2009;50:1423–1432.
63. Peters W, Cyster JG, Mack M, et al. CCR2-dependent trafficking of F4/80dim macrophages and CD11cdim/intermediate dendritic cells is crucial for T cell recruitment to lungs infected with Mycobacterium tuberculosis. *J Immunol.* 2004;172:7647–7653.

64. Fantuzzi L, Borghi P, Ciolli V, Pavlakis G, Belardelli F, Gessani S. Loss of CCR2 expression and functional response to monocyte chemotactic protein (MCP-1) during the differentiation of human monocytes: role of secreted MCP-1 in the regulation of the chemotactic response. *Blood.* 1999;94:875–883.
65. Sullivan R, Penfold P, Pow DV. Neuronal migration and glial remodeling in degenerating retinas of aged rats and in nonneovascular AMD. *Invest Ophthalmol Vis Sci.* 2003;44:856–865.
66. Marc RE, Jones BW, Watt CB, Vazquez-Chona F, Vaughan DK, Organisciak DT. Extreme retinal remodeling triggered by light damage: implications for age related macular degeneration. *Mol Vis.* 2008;14:782–806.
67. Penfold PL, Madigan MC, Gillies MC, Provis JM. Immunological and aetiological aspects of macular degeneration. *Prog Ret Eye Res.* 2001;20:385–414.
68. Espinosa-Heidmann DG, Suner IJ, Hernandez EP, Monroy D, Csaky KG, Cousins SW. Macrophage depletion diminishes lesion size and severity in experimental choroidal neovascularization. *Invest Ophthalmol Vis Sci.* 2003;44:3586–3592.
69. Combadiere C, Feumi C, Raoul W, et al. CX3CR1-dependent subretinal microglia cell accumulation is associated with cardinal features of age-related macular degeneration. *J Clin Invest.* 2007; 117:2920–2928.
70. Sakurai E, Anand A, Ambati BK, van Rooijen N, Ambati J. Macrophage depletion inhibits experimental choroidal neovascularization. *Invest Ophthalmol Vis Sci.* 2003;44:3578–3585.
71. Patel M, Chan CC. Immunopathological aspects of age-related macular degeneration. *Semin Immunopathol.* 2008;30:97–110.
72. Luhmann UF, Robbie S, Munro PM, et al. The drusenlike phenotype in aging Ccl2-knockout mice is caused by an accelerated accumulation of swollen autofluorescent subretinal macrophages. *Invest Ophthalmol Vis Sci.* 2009;50:5934–5943.
73. Tsutsumi C, Sonoda KH, Egashira K, et al. The critical role of ocular-infiltrating macrophages in the development of choroidal neovascularization. *J Leukoc Biol.* 2003;74:25–32.
74. Ambati J, Anand A, Fernandez S, et al. An animal model of age-related macular degeneration in senescent Ccl-2- or Ccr-2-deficient mice. *Nat Med.* 2003;9:1390–1397.